UDC 621.372.54

A. Zazerin, **A. Orlov**, Ph.D., **O. Bogdan**
National Technical University of Ukraine «Kyiv Polytechnic Institute»,
16 Polytechnichna Str., Kyiv, 03056, Ukraine.

Simplified thin film resonator model for high order filters application

The simplified model of thin film piezoelectric resonator based on multiloop equivalent circuits was developed and presented in this work. The model allows the straightforward integration of the resonator's electrical behavior into the most of modern CAD systems as a part of complex devices and enables the precise evaluation of the output characteristics in a relatively wide frequency range that is especially significant for the modelling of high-order filters composed of thin film bulk acoustic resonators. The model verification was given including: 1) the analysis of the absolute input impedance frequency dependence in wide and narrow frequency ranges; 2) the model agreement examination using different active layer and electrodes materials. An important advantage of proposed solution is the decreasing of calculation time and improving of optimization efficiency of complex RF circuits with a large number of resonators. References 8, figures 12, tables 1.

Keywords: *FBAR; SMR; thin film resonator; high-order filters Introduction.*

Introduction

In recent years the progress in the field of bulk acoustic wave (BAW) piezoelectric resonators has led to the possibility of manufacturing of frequency selective systems with features which enable the efficient exploitation in the frequency range up to 10 GHz. High quality factor and electromechanical coupling coefficient of these BAW resonators led to the great performance especially in terms of cutoff rate and out-of-band rejection ratio. Filters based on BAW resonators stand good for their low transmission loss (lower than 0.5 dB in comparison with SAW filters), moderate energy consumption (tens of microwatts) [1] and can be integrated with active elements on a single chip which makes them very promising option applied to mobile communication devices.

At the same time the calculation of the frequency-loss characteristics of the filter based on BAW resonators represents a complicated engineering challenge. The developed for today and commonly used solutions in the field of BAW resonators simulation include a variety of one-dimensional (BVD, Mason and its modifications Redwood and KLM) and three-dimensional physical models. The simplest Butterworth-Van-Dyke (BVD) model of resonator provides the electrical characteristics of the device in a narrow near-resonant frequency range, however it does not account for a variety of intrinsic real device effects. For instance the finite thickness of the electrodes leads to an eigenfrequency shift; the nonideal acoustic isolation and corresponding acoustic energy leakage reduce the effective bandwidth and quality factor.

On the other hand three-dimensional models which engage the finite element (FEM) calculation method allow estimating the characteristics of resonator with high precision taking into account even the edge reflection effects and arbitrary electrode geometry. A significant disadvantage of three-dimensional models is their calculation time and complexity of integration into modern RF circuit design software. Thus, in [2] the calculation of three-dimensional resonator with a circular step-like top electrode took more than 4 hours in COMSOL Multiphysics. In addition to above the output data suitable for application in CAD are typically standardized Touchstone files containing the frequency response of the device for a specific structural modification of the device. The features mentioned above seriously complicate the analysis of complex filters consisting of a large number of resonators and in fact eliminate the possibility of design parameters optimization.

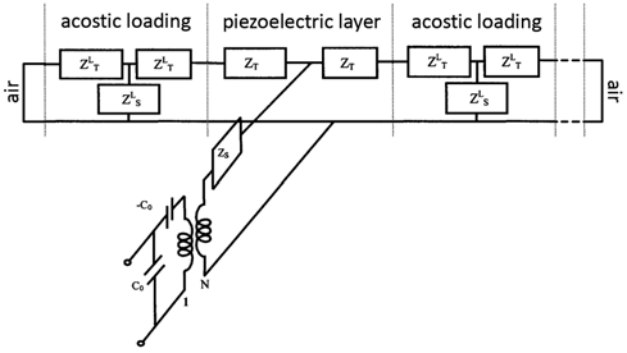

Fig. 1. Equivalent Mason circuit representation of the piezoelectric resonator with acoustic loading layers. The depicted device is given as mechanically unclamped which is modelled by short circuits at the air-solid interface

The Mason model composition concept (Fig. 1) is a compromise alternation which provides the ac-

counting of main effects of real devices. Due to its consistency and sequential structure the model is often used to simulate the multilayered structures such as trending solidly mounted resonators (SMR) with Bragg reflector as acoustic energy isolation method. However, as a distributed parameters model based on electrical transmission lines it requires the appropriate software simulation framework which was realized not in all CAD systems. After that the modelling of complex electronic circuits based on multilayered structures may be inefficient in many cases because of inexpediency of accounting for multipath acoustic wave propagation and rereflection in resonator layers.

The proposed method for simulation of thin film piezoelectric resonator is based on simplification of active layer's model and electrode's model in that way which enables the possibility of rapid adjustment of model accuracy and, accordingly, its calculation speed. The development of such an adaptive model allows one to apply it for effective evaluation and optimization of high-order filter parameters as well as for obtaining the final output frequency responses with high accuracy.

Piezoelectric layer model

To ensure the proper operation of bulk acoustic wave resonator the propagation of longitudinal waves should be enclosed by the volume of piezoelectric material. In other words the acoustic energy must be concentrated locally without leakage into other device parts. The acoustic energy localization can be performed by introducing the discontinuities into the acoustic wave propagation path, so that the latter is reflected. The most effective discontinuity is the air–solid material interface which is implemented in film bulk acoustic resonators (FBAR) design. Another approach is to create a periodic Bragg reflector used in SMR-type devices. SMR resonators have advantages of less sensitivity to reciprocal layers tension, manufacturability, improved thermal conductivity and mechanical strength [3]. The downside of this approach is the low quality factor and electromechanical coupling coefficient as any additional layers in resonator structure act as mass loading. For this reason membrane-type resonators are still widely used in a variety of filters, duplexers and oscillators [4].

The arbitrary thin film membrane piezoelectric resonator depicted in Figure 2. It is represented by piezoelectric layer material sandwiched between two electrodes. Acoustic isolation is implemented as the air-solid interfaces above the top electrode and below the bottom one.

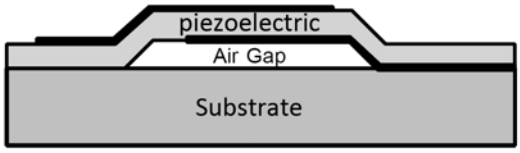

Fig. 2. Arbitrary scaled membrane–type BAW resonator design

In accordance with Mason's approach piezoelectric layer of the resonator is represented by T-shaped section (Fig. 1) with impedances Z_T, Z_S and series of capacitor C_0 and transformer that simulates the electroacoustic conversion in piezomaterial. The total acoustic loading of a resonator can be represented by two impedances Z_{TE} и Z_{BE} loaded onto the top and bottom interfaces of the active layer and comprising the acoustic impedances of the electrodes and any additional layers including Bragg reflector. The equivalent circuit of the model in this case can be simplified as shown in the figure below:

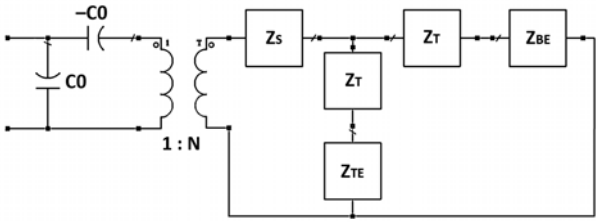

Fig. 3. Simplified circuit of the resonator with acoustic loadings Z_{TE} and Z_{BE}

where the following designations is given:

$$C_0 = \frac{\varepsilon_0 \varepsilon_s^{33} A}{D_a}, \qquad Z_S = -jZ_0 / \sin(2\varphi),$$

$$Z_0 = A\rho_a V_a, \qquad Z_T = jZ_0 \tan(\varphi),$$

$$N = C_0 h_{33} = C_0 \frac{e^{33}}{\varepsilon_0 \varepsilon_s^{33}}, \qquad \varphi = \frac{\pi D_a f}{V_a}.$$

Such a scheme can be redrawn using the procedure described in [5, p. 135–137]. According to the mentioned algorithm, L-shaped part of the circuit can be replaced by the reversed in direction L-shaped circuit with a transformer as shown in Fig.4.

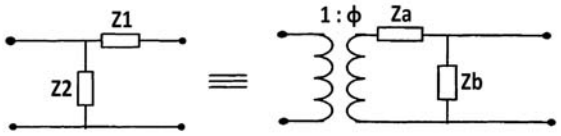

Fig. 4. Equivalence of an L-shaped network with a corresponding reversed L-shaped network with transformer

$$Z_a = \frac{Z_1}{Z_2}\left(Z_1 + Z_2\right), \quad (1)$$

$$Z_b = Z_1 + Z_2, \quad (2)$$

$$\phi = 1 + \frac{Z_1}{Z_2}, \quad (3)$$

where Z_a and Z_b are the new equivalent impedances and φ – transformation coefficient of the transformer. The model can be simplified to the form shown in Figure 5 using this methodology.

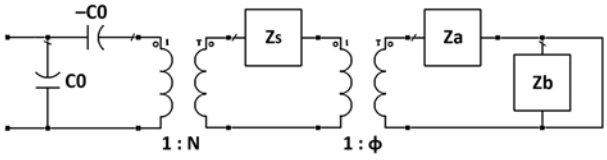

Fig. 5. Equivalent circuit representation of the model after employing the L-shaped network replacement technique

Whereby the values of the new equivalent impedances and conversion ratio of the transformer are described by the following expressions:

$$Z_a = \frac{Z_T + Z_{BE}}{Z_T + Z_{TE}}\left(2Z_T + Z_{TE} + Z_{BE}\right), \quad (4)$$

$$Z_b = 2Z_T + Z_{TE} + Z_{BE}, \quad (5)$$

$$\phi = 1 + \frac{Z_T + Z_{BE}}{Z_T + Z_{TE}}. \quad (6)$$

The result of such replacement of L-shaped network becomes the shunt of equivalent impedance Z_b which eliminates this element out of the circuit. What is most remarkable is the frequency behavior of the relationship represented in Figure 6. In view of the prevalence of the impedance Z_T in a wide near-resonant frequency range the ratio $(Z_T+Z_{BE})/(Z_T+Z_{TE})$ takes a value close to 1 which allows one to significantly simplify the expressions (4), (6) and obtain the conversion ratio of the second transformer that equals two. In this case the transformer loading becomes the series of impedances $2Z_T + Z_{TE} + Z_{BE}$ (Fig. 7).

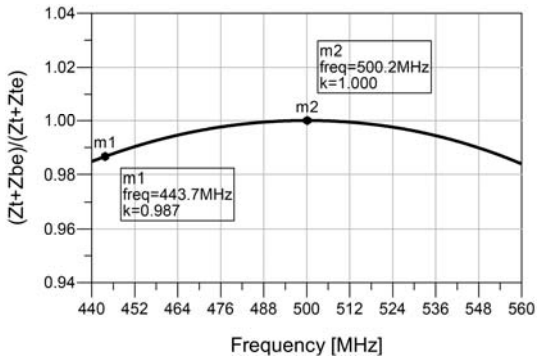

Fig. 6. Frequency behavior of $(Z_T+Z_{BE})/(Z_T+Z_{TE})$ in near-resonant frequency range

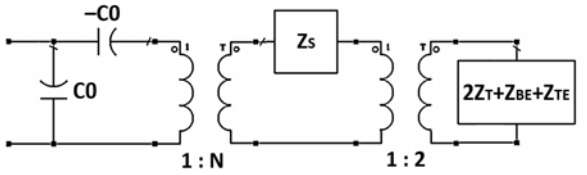

Fig. 7. Simplification of equivalent circuit in near-resonant frequency range

Further simplification of the model boils down to transfer of impedance Z_S to the right part of the circuit and the union of two transformers (Fig. 8).

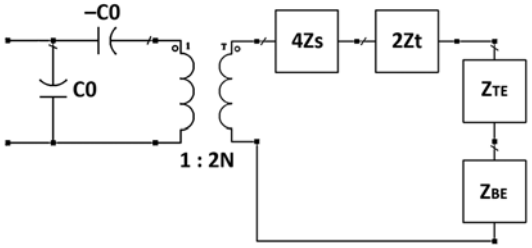

Fig. 8. The equivalent circuit after the union of transformers

Now let us consider in detail the series of impedances in Figure 8, assuming:

$$Z_{eq} = 4Z_S + 2Z_T, \quad (7)$$

$$Z_{eq} = \frac{-4jZ_0}{\sin(2\varphi)} + 2jZ_0\tan(\varphi) = 2Z_0\coth(j\varphi). \quad (8)$$

Herewith the admittance takes the form $Y_{eq} = \frac{1}{2Z_0}\tanh(j\varphi)$ and can be expanded in a series for the hyperbolic tangent function [6]:

$$\tanh(\gamma) = \sum_{k=0}^{\infty}\frac{8\gamma}{(2k+1)^2\pi^2 + 4\gamma^2} = \frac{8\gamma}{\pi^2 + 4\gamma^2} + \frac{8\gamma}{9\pi^2 + 4\gamma^2} + \ldots \quad (9)$$

The equation (9) can be schematically represented as an infinite number of parallel combinations of capacitors and inductors connected in series. The corresponding values of C_n and L_n can be found as the solution of the following equation:

$$\frac{8j\varphi}{(2k+1)^2\pi^2-4\varphi^2}=\frac{j\omega C}{1-\omega^2 L_n C_n}, \quad (10)$$

$$L_n=\frac{Z_0 D_a}{2V_a}, \quad (11)$$

$$C_n=\frac{2D_a}{(2k+1)^2\pi^2 Z_0 V_a}. \quad (12)$$

There are three possible energy losses mechanisms in piezoelectric layers associated with mechanical, dielectric and piezoelectric effects. Among them the mechanical losses are of the greatest impact near the resonance [7] and are due to the delay between the strain and the applied force (hysteresis effect). Mechanical quality factor of the resonator is defined as the ratio of stress in phase with strain velocity to the stress out of phase with strain velocity. The electrical counterparts of stress and velocity are voltage and current, so the quality factor of the equivalent circuit is defined as the ratio of reactance to resistance. Hence for the series RLC circuit one can obtain:

$$Q_m=\frac{imag(Z)}{real(Z)}=\sqrt{\frac{L_n}{C_n}}\frac{1}{R_n}. \quad (13)$$

Consequently the value of mechanical quality factor can be taken into account in the model by introducing the additional resistance in series network that is described by the next expression:

$$R_n=\sqrt{\frac{L_n}{C_n}}\frac{1}{Q_m}=\frac{\pi(2k+1)Z_0}{2Q_k}, \quad (14)$$

where Q_k is the quality factor of the resonator at each corresponding resonant frequency.

Thus, the equivalent circuit of the resonator can be redrawn in the way depicted in Figure 9.

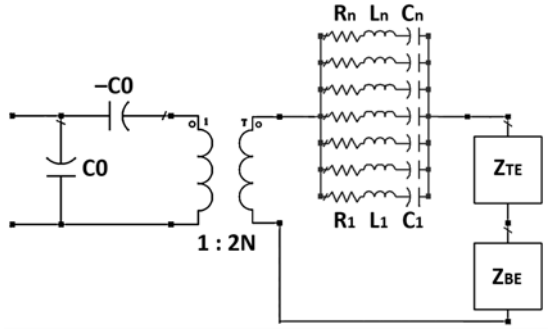

Fig. 9. Equivalent circuit of the resonator model with simplified active layer section

Electrode layer model

In a real device the piezoelectric material layer is enclosed between two metal electrodes placed on the top and bottom faces of the resonator. In case of SMR design a bunch of Bragg reflector layers is also added. Such a loading of the piezoelectric layer leads to several mechanical and electrical effects known as mass-loading effects. These effects are responsible for the resonance frequency shift and reduction of effective frequency bandwidth of the resonator and hence should be taken into account in the equivalent model.

The acoustic impedance of the metal electrode can be found as a solution of an analytical expression for a single T-shaped loading section (Fig. 1):

$$Z_{el}=Z_e\frac{Z_{load}+Z_e\tanh(j\varphi_{el})}{Z_e+Z_{load}\tanh(j\varphi_{el})}, \quad (15)$$

where Z_e is the characteristic impedance of the electrode layer, Z_{load} is the loading impedance and phase $\varphi_{el}=\frac{2\pi f D_{el}}{V_{el}}$.

The acoustic loading of electrode can be an air gap (Z_{load}~0), that corresponds to the simple case of FBAR design or Bragg reflector in case of SMR. A notable feature of the Brag reflector is its very low impedance near the resonant frequency that allows one to simplify the expression (15) for the acoustic impedance:

$$\lim_{Z_{load}\to 0}(Z_{el})=Z_e\tanh(j\varphi_{el}). \quad (16)$$

Herewith the admittance takes the form $Y_{el}=\frac{1}{Z_e}\coth(j\varphi_{el})$ and can be expanded in a series for the hyperbolic cotangent function:

$$\coth(\gamma)=\frac{1}{a}+\sum_{l=1}^{\infty}\frac{2\gamma}{l^2\pi^2+\gamma^2}=\\ =\frac{1}{a}+\frac{2\gamma}{\pi^2+\gamma^2}+\frac{2\gamma}{4\pi^2+\gamma^2}+\ldots \quad (17)$$

The equation (17) can be schematically represented as an inductor and an infinite number of parallel combinations of capacitors and inductors connected in series. The corresponding values of L, C_m and L_m can be found as the solution of the following equation:

$$\frac{1}{j\varphi_{el}}+\frac{2j\varphi_{el}}{l^2\pi^2-\varphi_{el}^2}=\frac{1}{i\omega L}+\frac{j\omega C}{1-\omega^2 L_m C_m}, \quad (18)$$

$$L = \frac{Z_e D_{el}}{V_{el}}, \quad (19)$$

$$L_m = \frac{Z_e D_{el}}{8 V_{el}}, \quad (20)$$

$$C_m = \frac{2 D_{el}}{Z_e l^2 \pi^2 V_{el}}. \quad (21)$$

In case of FBAR resonator design the value Z_e should be doubled for the simulation of both top and bottom electrodes. The complete equivalent circuit of thin film piezoelectric resonator which accounts mass-loading effect of electrodes is shown in Figure 10.

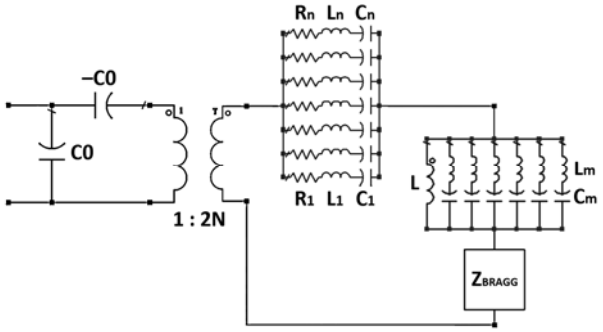

Fig. 10. Complete equivalent circuit of the resonator model including multiloop networks of active layer and electrodes. Impedance Z_{BRAGG} shown as opportunity example for further model development

It is worth mentioning that the developed model allows one to define accuracy to calculation speed ratio by changing the number of parallel RLC circuits. Such a flexibility can be applied at various stages of filter development. The possibility of series connection of acoustic loadings can be exploited in future as the model adaptation for complex SMR-type resonators by simply adding the Bragg reflector's frequency dependent impedance model.

Model validation

The verification of practical characteristics of thin film piezoelectric resonator model was carried out by a comparative analysis of the total input impedance frequency dependence. In this case the standard Mason approach for the membrane-type structure (Fig. 2) was chosen as a reference model. The model's frequency behavior and simulation accuracy were under consideration along with its coherence under variation of frequently used piezoelectric and electrode materials. Al, Ti, Mo, Au with thickness of 200 nm were used as the electrodes, while AlN, ZnO and PZT were used as active layer with a thickness corresponding to the operation frequency of 500 MHz. Seven parallel circuits in both active layer model and electrode model were used in simulations.

The normalized root mean square error (NRMSE) was chosen as a model consistency criteria. It is often used to compare models outputs [8] and can be calculated using the following expression:

$$NRMSE = 1 - \frac{\|Z_{ref} - Z_{test}\|}{\|Z_{ref} - mean(Z_{ref})\|}, \quad (22)$$

where || indicates the 2-norm of a vector (Euclidean norm), Z_{ref} – the output data set of the reference model, Z_{test} – the output data set of the test model. The NRMSE criteria value varies between –∞ (bad fit) to 1 (perfect fit).

It is worthy of note that the following results were obtained using the MatLab numerical computing environment and Agilent Advanced Design System for electronic circuit simulations. In particular, but not limited to this point, the frequency dependence of the resonator's input impedance in case of AlN with aluminum electrodes is shown in Figure 11.

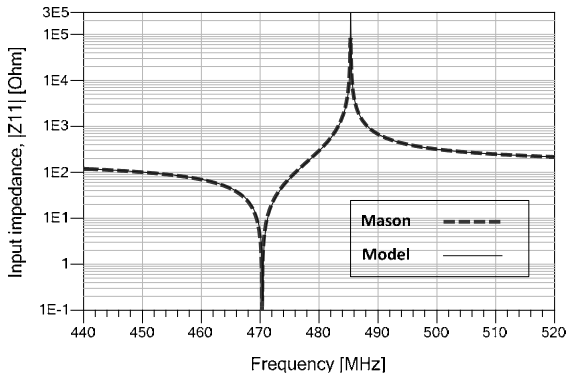

a)

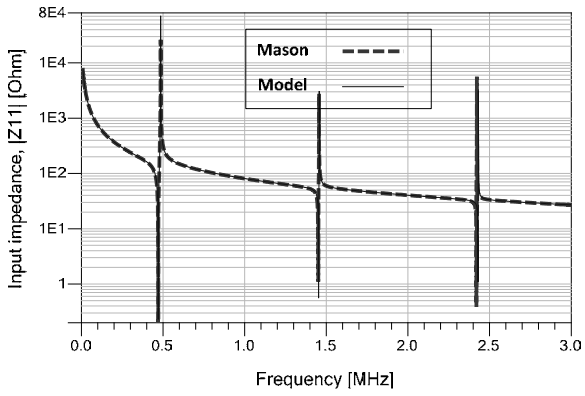

b)

Fig. 11. The comparison of absolute input impedance frequency dependence of reference model and presented model of the FBAR resonator in a narrow near-resonant (a) and wide (b) frequency ranges

As proceeding from the presented simulation results the developed model has high agreement accuracy with the reference model in a narrow near-resonant frequency range as well as in wide band. Whereby the simulation of eigenfrequency shift due to electrodes mass-loading (485 MHz instead of 500 MHz in unclamped active layer) and the natural periodicity of higher harmonics were provided. The mechanical quality factor was introduced through the inclusion of additional resistances in active layer equivalent circuit.

The calculation results of the frequency response fit for different active layer and electrode materials are listed in Table 1. The table contains data for narrow near-resonant Δf_{local}: 440-520 MHz and wide frequency band Δf_{wide}: 0.1-1000 MHz.

Table 1. Model consistency for different active layer and electrode materials.

Material combinations	NRMSE @Δf_{local}	NRMSE @Δf_{wide}
AlN–Al	-0,526	-0,235
AlN–Ti	-1,31	-1,160
AlN–Mo	-0,197	-0,09
AlN–Au	-0,839	-0,544
ZnO–Al	0,02	0,02
PZT–Al	0,332	0,335

According to the listed data the divergence rate varies slightly for different materials while maintaining acceptable resonator's frequency response accuracy. In the narrow near-resonant frequency range the accuracy of the model was slightly degraded as a result of the introduced mechanical quality factor. As expected, the application of different electrode materials in resonator structure has led to remarkable resonant frequency shifts (Fig. 12).

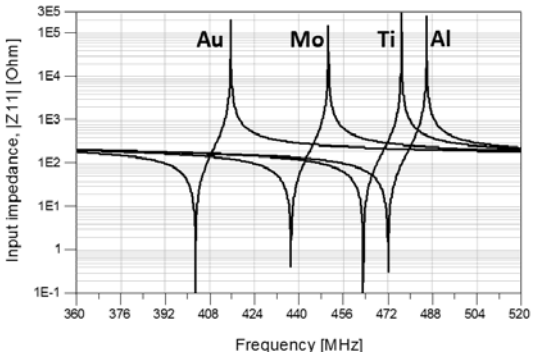

Fig. 12. The calculated results of the impedance for the FBARs with different electrodes

The performed analysis of the developed model performance in terms of total input impedance calculation showed a more than double decreasing of calculation time in comparison to reference Mason model using Agilent ADS environment.

Conclusions

The paper presents a simplified lumped element thin film piezoelectric resonator model based on multiloop equivalent circuits of active layer and electrodes. The model validation including the frequency response analysis for different comprising materials proved the model's applicability to evaluate the output characteristics of the resonator in longitudinal wave mode. Presented approach allows one to calculate the resonant frequency shift while using different electrode thicknesses and materials. The introduction of the finite mechanical quality factor of the resonator opens the possibility of evaluation the energy losses in the device. In a wide frequency range the model provides the simulation of higher harmonics which are especially critical in the design of wideband filters. However, the most important advantage of the presented solution is the possibility of its quick reconfiguration based on the variation of equivalent networks complexity: from the time-efficient model with low accuracy to a complicated circuit that is not inferior to Mason model in terms of accuracy. As a consequence, the model can be integrated into the most of modern CAD systems and used both for rapid calculation and optimization of design parameters of high-order filters and for obtaining the final output frequency responses with high accuracy.

References

1. *Nelson A. et al.* (2011), A 22μW, 2.0GHz FBAR oscillator. IEEE Radio Frequency Integrated Circuits Symposium (RFIC). Baltimore, MD: IEEE, Pp. 1–4.
2. *Yakimenko Y. et al.* (2014), Film bulk acoustic resonator finite element model in active filter design. Proceedings of the 37th International Spring Seminar on Electronics Technology (ISSE). Dresden: IEEE, Pp. 486–490.
3. *Hashimoto K.* (2009), RF Bulk Acoustic Wave Filters for Communications. 1 edition. London: Artech House Publishers, P. 275.
4. *Ruby R. et al.* (2001), Ultra-miniature high-Q filters and duplexers using FBAR technology. IEEE Solid-state circuits international confer-

ence. Digest of Technical Papers. ISSCC. Pp.120–121.
5. *Shea T.E.* (1929), Transmission networks and wave filters. Princeton, N.J., D. Van Nostrand, P. 470.
6. *Harris J.W., Stöcker H.* (1988), Handbook of Mathematics and Computational Science. NewYork: Springer-Verilog, P.1028.
7. *Poplavko Y.M., Pereverzeva L.P., Raevski I.P.* (2009), Physics of Active Dielectrics. Rostov: Publishing of South Federal University. P.480.
8. *Granderson J., Price P.* (2012), Evaluation of the Predictive Accuracy of Five Whole Building Baseline Models. Lawrence Berkley National Laboratory.

Поступила в редакцию 10 ноября 2014 г.

УДК 621.372.54

А.І. Зазерін, **А.Т. Орлов**, канд. техн. наук, **А.В. Богдан**
Національний технічний університет України "Київський політехнічний інститут",
вул. Політехнічна, 16, корпус 12, Київ, 03056, Україна.

Спрощена модель тонкоплівкового резонатора для застосування у фільтрах високого порядку

У роботі представлена розроблена авторами модель тонкоплівкового п'єзоелектричного резонатора з двома електродами, заснована на застосуванні багатоконтурних схем заміщення. Завдяки спрощеності структури, дана модель може бути легко інтегрована в більшість сучасних САПР і дозволить з високою точністю визначати вихідні характеристики резонатора у відносно широкому частотному діапазоні, що особливо важливо при моделюванні фільтрів високого порядку на базі резонаторів. Проведена верифікація моделі, що включає аналіз частотної залежності вхідного імпедансу у вузькому і широкому частотних діапазонах, а також дослідження узгодженості моделі при використанні різних матеріалів активного шару і електродів. Важливою перевагою запропонованої моделі є збільшення ефективності розрахунку та оптимізації складних схем із застосуванням великої кількості резонаторів за рахунок скорочення часу розрахунку. Бібл. 8, рис. 12, табл. 1.

Ключові слова: *FBAR; SMR; тонкоплівковий резонатор; фільтри високого порядку.*

.

УДК 621.372.54

А.И. Зазерин, **А.Т. Орлов**, канд. техн. наук, **А.В. Богдан**
Национальный технический университет Украины «Киевский политехнический институт»,
ул. Политехническая, 16, корпус 12, г. Киев, 03056, Украина.

Упрощенная модель тонкопленочного резонатора для применения в фильтрах высокого порядка

В работе представлена разработанная авторами модель тонкопленочного пьезоэлектрического резонатора с двумя электродами, основанная на применении многоконтурных схем замещения. Благодаря упрощенности структуры, данная модель может быть легко интегрирована в большинство современных САПР и позволит с высокой точностью определять выходные характеристики резонатора в относительно широком частотном диапазоне, что особенно важно при моделировании фильтров высокого порядка на базе резонаторов. Проведена верификация модели, включающая анализ частотной зависимости входного импеданса в узком и широком частотных диапазонах, а также исследование согласованности модели при использовании различных материалов активного слоя и электродов. Важным преимуществом предложенной модели является увеличение эффективности расчета и оптимизации сложных схем с применением большого количества резонаторов за счет сокращения времени расчета. Библ . 8, рис. 12, табл. 1.

Ключевые слова: *FBAR; SMR; thin film resonato; high-order filters.*

Список использованных источников

1. *Nelson A. et al.* A 22μW, 2.0GHz FBAR oscillator // IEEE Radio Frequency Integrated Circuits Symposium (RFIC). Baltimore, MD: IEEE, 2011. P. 1–4.
2. *Yakimenko Y. et al.* Film bulk acoustic resonator finite element model in active filter design // Proceedings of the 37th International Spring Seminar on Electronics Technology (ISSE). Dresden: IEEE, 2014. P. 486–490.
3. *Hashimoto K.* RF Bulk Acoustic Wave Filters for Communications. 1 edition. London: Artech House Publishers, 2009. 275 p.
4. *Ruby R. et al.* Ultra-miniature high-Q filters and duplexers using FBAR technology // IEEE Solid-state circuits international conference. Digest of Technical Papers. ISSCC. 2001. P. 120–121.
5. *Shea T.E.* Transmission networks and wave filters. Princeton, N.J., D. Van Nostrand, 1929. 470 p.
6. *Harris J.W., Stöcker H.* Handbook of Mathematics and Computational Science. NewYork: Springer-Verilog, 1998. 1028 p.
7. *Poplavko Y.M., Pereverzeva L.P., Raevski I.P.* Physics of Active Dielectrics. Rostov: Publishing of South Federal University, 2009. 480 p.
8. *Granderson J., Price P.* Evaluation of the Predictive Accuracy of Five Whole Building Baseline Models. Lawrence Berkley National Laboratory, 2012.